Biochemistry
Communication
Cite This: Biochemistry XXXX, XXX, XXX−XXX
pubs.acs.org/biochemistry

Overexpression of Osmosensitive Ca^{2+}-Permeable Channel TMEM63B Promotes Migration in HEK293T Cells

Marta C. Marques,*[,†,§] Inês S. Albuquerque,[†,§] Sandra H. Vaz,[†] and Gonçalo J. L. Bernardes*[,†,‡]

[†]Instituto de Medicina Molecular, Faculdade de Medicina, Universidade de Lisboa, Avenida Professor Egas Moniz, 1649-028 Lisboa, Portugal

[‡]Department of Chemistry, University of Cambridge, Lensfield Road, Cambridge CB2 1EW, U.K.

Supporting Information

ABSTRACT: The recent discovery of the osmosensitive calcium (Ca^{2+}) channel OSCA has revealed the potential mechanism by which plant cells sense diverse stimuli. Osmosensory transporters and mechanosensitive channels can detect and respond to osmotic shifts that play an important role in active cell homeostasis. Members of the TMEM63 family of proteins are described as the closest homologues of OSCAs. Here, we characterize TMEM63B, a mammalian homologue of OSCAs, recently classified as mechanosensitive. In HEK293T cells, TMEM63B localizes to the plasma membrane and is associated with F-actin. This Ca^{2+}-permeable channel specifically induces Ca^{2+} influx across the membrane in response to extracellular Ca^{2+} concentration and hyperosmolarity. In addition, overexpression of TMEM63B in HEK293T cells significantly enhanced cell migration and wound healing. The link between Ca^{2+} osmosensitivity and cell migration might help to establish TMEM63B's pathogenesis, for example, in cancer in which it is frequently overexpressed.

More than 1000 families of transport proteins have already been recognized according to the IUBMB-approved Transporter Classification Database.[1] Recently, a new anoctamin (ANO) superfamily of Ca^{2+}-activated ion channels has been identified, which includes anoctamins (lipid scramblases), transmembrane channels (TMCs), and Ca^{2+}-permeable stress-gated cation channel (CSC) families.[2] Within this superfamily is the CSC-like family TMEM63, which shares the same topologies as the CSC family.[3] The lack of information about the molecular nature of the TMEM63 family encouraged us to investigate these ion channels.

Numerous proteins, such as *At*OSCA1.1 and *At*CSC1-OSCA1.2, found in *Arabidopsis thaliana* have been identified as mechanosensitive and structurally characterized.[4−6] In mammals, some cation channels have been proposed to mediate osmosensory transduction through proportional modulation of their probability of opening during changes in fluid osmolality, but the molecular identity of these channels remains unknown.[7] Among these are the OSCA orthologues, the TMEM63 family, proposed as likely candidates for the mammalian central osmosensory transduction pathway.[8] Interestingly, a recent study has linked OSCA/TMEM63A and -B channels to a mechanosensory role.[9] Investigation of the conserved domain architecture among these transporters revealed the existence of orthologs present in various taxonomic groups, such as fungi, green algae, plants, birds,

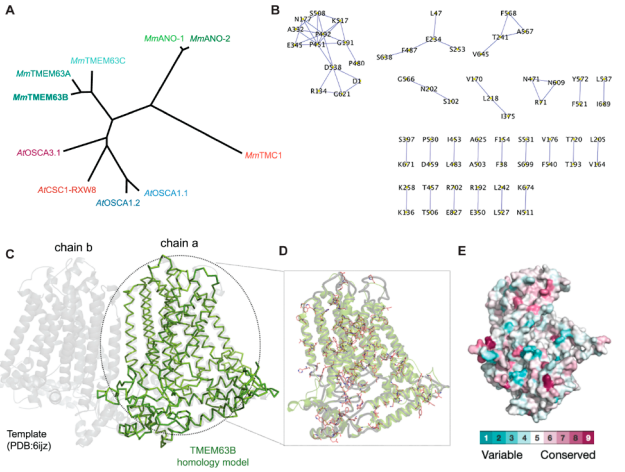

Figure 1. TMEM63B is an evolutionarily conserved protein that shares 3D homology with OSCA1. (A) Bayesian tree of proteins that are similar to the TMEM63 family (teal clade), OSCA1 (blue clade), CSC1 (magenta clade), OSCA3 (purple clade), TMC (red clade), and TMEM16 (green clade), all from *M. musculus*. The tree was generated in DrawTree.[15] (B) Co-evolution residue network analysis of 10 homologous proteins of *M. musculus* TMEM63B. The analysis was performed with CAPS[16] software to study co-evolving amino acids. Co-evolving amino acid pairs were defined in terms of their statistical support (defined as bootstrap values); only pairs with bootstrap values of >0.8 were used for the construction of networks with Cytoscape software.[17] (C) 3D homology model of the mouse TMEM63B protein in green, represented as a ribbon built with OSCA 1.2 as a template (PDB entry 6ijz), represented in gray as a cartoon by using Pymol.[18] (D) Partial representation of *Mm*TMEM63B (green) with the predicted 3D location of the conserved residues (pink element sticks). (E) ConSurf analysis for the homology model built with Modeler[19] for TMEM63B. The 3D structure is rendered as a surface and color-coded by its conservation grade by using the color-coding bar shown in the figure, with turquoise through bordeaux that indicates the variable to conserved residues. The analysis was carried out with MAFFT multiple-sequence alignment[12] available, and the figures were generated with the help of a PyMOL[18] script output by ConSurf.[20]

Received: March 15, 2019
Revised: June 14, 2019
Published: June 18, 2019

DOI: 10.1021/acs.biochem.9b00224
Biochemistry XXXX, XXX, XXX−XXX

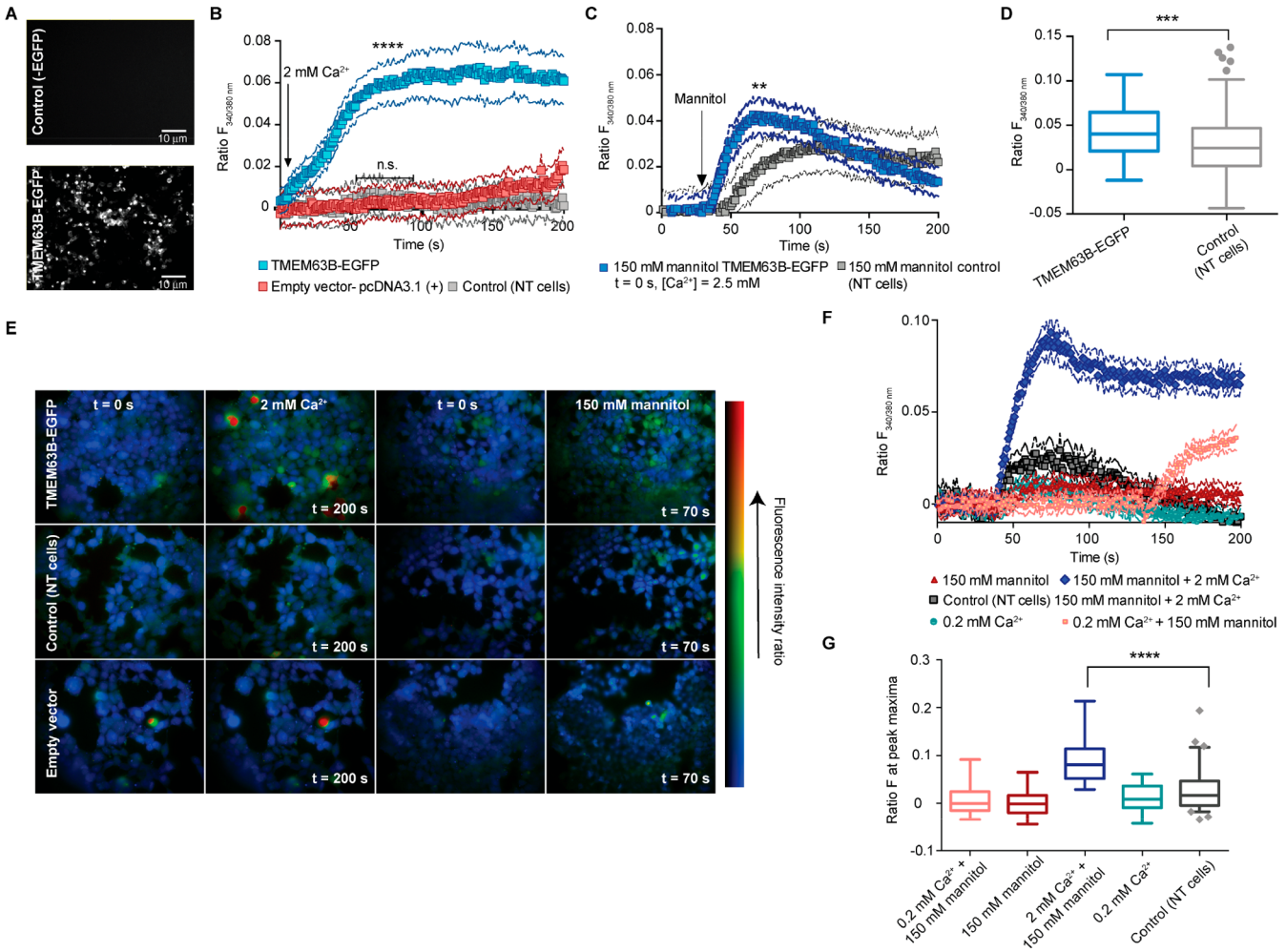

Figure 2. TMEM63B promotes $[Ca^{2+}]_i$ influx across the plasma membrane in response to extracellular $[Ca^{2+}]$ and hyperosmolarity. (A) Representative fluorescent images showing the HEK293T cells either nontransfected or transfected and showing an EGFP-positive signal. Scale bars represent 10 μm. (B) Increase in calcium influx induced by extracellular Ca^{2+} (2 mM) in EGFP-positive HEK293T cells. For quantification, the strongest responding cells were analyzed in each well (20−30 cells; $n = 3$) and normalized to the baseline. ****Mann−Whitney of unpaired t test data: significant difference between the empty vector and TMEM63B-EGFP ($p < 0.0001$) after peak determination by the analysis of the area under the curve. No significant difference between control and NT. (C) Increase in calcium influx induced by extracellular mannitol (150 mM) in EGFP-positive HEK293T cells. For quantification, the strongest responding cells were analyzed in each well (20−30 cells; $n = 3$) and normalized to the baseline. **Mann−Whitney of unpaired t test data between TMEM63B-EGFP and the control (NT cells) ($p < 0.0002$) at peak maxima. (D) Box plot of peaks at 70 s post-mannitol stimulation of HEK293T cells (control, NT cells). ***Mann−Whitney of unpaired t test data: significant difference between NT cells and TMEM63B-EGFP ($p < 0.0001$). (E) Calcium imaging of HEK293T cells transfected with the mouse TMEM63B-EGFP fusion protein or a pcDNA3.1(+) empty vector and nontransfected, corrected for baseline level before and after calcium (2 mM) or mannitol stimuli (150 mM) (color code, blue for a low calcium level, green for intermediate, yellow for medium high, and red for high). (F) Calcium influx induced by extracellular Ca^{2+} (0.2 and 2 mM) with a constant mannitol concentration of 150 mM. For quantification, the strongest responding cells were analyzed in each well ($n = 30$ cells) and normalized to the baseline. For the condition in which we used 0.2 mM Ca^{2+} and 150 mM mannitol (salmon symbols), we applied a second mannitol shock at 120 s. (G) Box plot of peaks after either calcium or mannitol stimulation at peak maxima. ****Mann−Whitney of unpaired t test data: significant difference between NT cells and TMEM63B-EGFP upon stimulation with 150 mM mannitol and 2 mM Ca^{2+} ($p < 0.0001$). NT cells, nontransfected cells. Values represent means ± the standard error of the mean.

and mammals, which suggests the functional conservation of this family throughout higher eukaryotes. With the availability of sequences of various ANO superfamily members and the recently reported three-dimensional (3D) structures of some OSCA proteins in *A. thaliana*,[4−6] it is possible to gain insight into the structural aspects of TMEM63B domains involved in ion translocation across the membrane.

By using BLAST[10] software, we performed similarity searches with *Mus musculus* TMEM63B (*Mm*TMEM63B) as the query protein (Uniprot entry Q3TWI9) against protein structures in the Protein Data Bank (PDB).[11] The protein with the highest alignment score (Table S1) corresponds to *A. thaliana* CSC1 (OSCA1.2), followed by *At*OSCAs 3.1 and 1.1. The bioinformatic analysis of the *Mm*TMEM63B amino acid sequence showed the presence of three different domains, a cytoplasmic PHM7 cyt domain and a N-terminal and C-terminal Ca^{2+}-dependent channel domain (RSN1), which consists of a total of 11 transmembrane (TM) predicted regions (Figure S1). We selected 10 representative members of the ANO superfamily and performed a multiple-sequence alignment with the MAFFT 7 program[12] (Figure S2) to identify functionally and structurally conserved residues and built a phylogenetic tree (Figure 1A). The structure and function of a protein rely on coordinated interactions among

DOI: 10.1021/acs.biochem.9b00224
Biochemistry XXXX, XXX, XXX−XXX

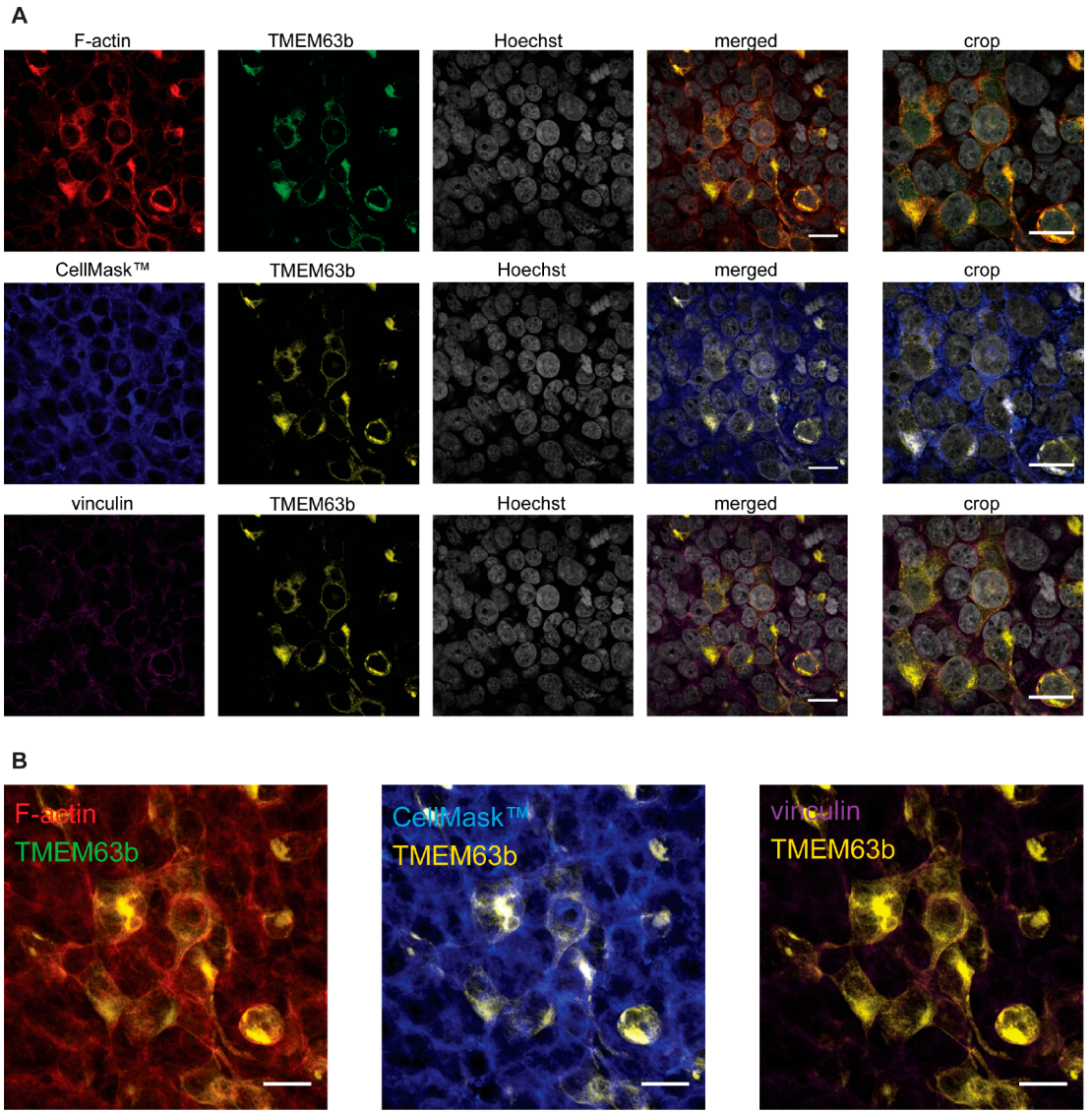

Figure 3. TMEM63B localizes to the membrane and co-localizes with cortical F-actin but not with vinculin. (A) Confocal microscopy images of 6 μm optical slices of fixed HEK293T cells transfected with TMEM63B-EGFP and stained with phalloidin (red), CellMask Plasma membrane stain (blue), anti-vinculin (magenta), and Hoechst 33342 (gray). In the right panel, we show a crop of the merged channels, to further accent co-localization or the lack thereof between these markers and *Mm*TMEM63B. *Mm*TMEM63B is colored either green or yellow. (B) Z projection of the merged channels, corresponding to the same imaged fields shown above. Scale bars represent 10 μm. Co-localization analysis (Pearson's coefficient): for TMEM63B vs vinculin, $r = 0.039$; for TMEM63B vs F-actin, $r = 0.701$; for TMEM63B vs the cell membrane $r = 0.393$, showing partial co-localization with the cell membrane and F-actin but not with vinculin.

its residues.[13] Therefore, the relationship of other structural features of TMEM63B residues could be determined through the identification of residues that co-vary with each other during evolution. We have found several residues with higher connectivity in the network (Figure 1B and Table S2), such as P492, P451, S508, D538, N177, K517, E345, and A332, which are also residues with a high degree of conservation. To produce a model of the TMEM63B tertiary structure, the *At*CSC1-OSCA1.2 3D structure was selected as a template for homology modeling by using the SWISS-MODEL server.[14] The OSCA1.2 structure and predicted TMEM63B 3D model appear to share a similar 3D fold (Figure 1C). In the obtained homology model, it is possible to observe several helices and a smaller number of strands that are localized within conserved regions of OSCA proteins, in agreement with the bioinformatic predictions. The computed degree of conservation for each residue was then mapped onto the predicted model of TMEM63B (Figure 1C,D and Table S3). The conserved patches essentially fall in TM1, TM4−TM7, TM9, and TM10. The cytosolic domains of OSCAs comprise a RNA recognition motif (RRM)[4,6] that is also present in TMEM63B (Figure S3A). On the basis of an intensive search for similar sequences by using the SWISS-MODEL server[14] and PDB,[11] we identified three consensus sequences (see Figure S3B) that are conserved in TMEM63A and -B and a family of RNA binding proteins, the heterogeneous nuclear ribonucleoprotein A1 (hnRNP A1, PDB entry 4yoe) and U6 snRNP binding protein (PDB entry 2do4). However, the capability of TMEM63B to bind RNA remains undetermined and should be investigated in future studies.

The putative ion conduction pore and the mechanosensitive features of OSCAs structures were shown to be partially

DOI: 10.1021/acs.biochem.9b00224
Biochemistry XXXX, XXX, XXX−XXX

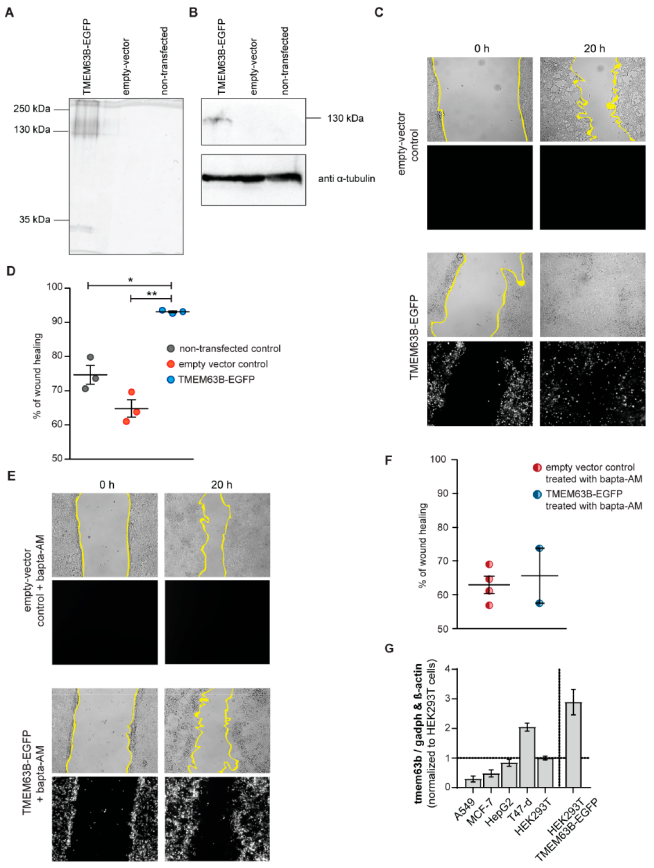

Figure 4. TMEM63B overexpression in HEK293T enhances cell migration in a calcium-dependent manner. (A) Whole HEK293T cell lysates were assayed on a 10% sodium dodecyl sulfate gel with fluorescence imaging with a Typhoon fluorescence scanner (excitation with a 488 nm laser) and (B) Western blot. Cell lysates from controls (empty vector and nontransfected cells) and *Mm*TMEM63B-EGFP cells were quantified, and 50 μg from each protein extract was loaded on a 10% sodium dodecyl sulfate−polyacrylamide gel electrophoresis gel, as indicated. The sodium dodecyl sulfate gel was imaged on a Typhoon scanner and then transferred to a polyvinylidene fluoride membrane. (C) Representative transmitted-light wide-field microscopy images of cells transfected with an empty vector or with *Mm*TMEM63B-EGFP. Images were taken as soon as the scratch was performed (0 h) or, at the same position, after 20 h. (D) Quantification of the percentage of wound healing in a 20 h scratch assay. Bars indicate averages, and error bars indicate standard errors of the mean. (E) Representative transmitted-light wide-field microscopy images of cells transfected with an empty vector or *Mm*TMEM63B-EGFP and incubated with bapta-AM, a known Ca^{2+} chelator. Images were taken as soon as the scratch was performed (0 h) or, at the same position, after 20 h. (F) Quantification of the percentage of wound healing in a 20 h scratch assay when cells were treated with bapta-AM. Statistical analysis was performed with a two-tailed unpaired *t* test with Welch's correction (**p < 0.02, and *p < 0.05). (G) Quantification of mRNA levels of hTMEM63B in human tumor cell lines by quantitative real-time polymerase chain reaction. Data shown as ΔΔCT of tmem63b to housekeeping genes gadph and β-actin, normalized to ΔCT for HEK293T cells.

conserved in TMEM63B (Figure S3B). On the basis of these data and under the assumption that TMEM63 proteins could be osmosensitive calcium-activated channels, we decided to clone the TMEM63B gene from *M. musculus*, fused to enhanced green fluorescent protein (EGFP), and overexpress it in human embryonic kidney 293 (HEK293T) cells. We confirmed the TMEM63B-EGFP construct expression (Figure 2A) and loaded cells with the calcium-responsive dye Fura-2AM. Stimulation with 2 mM Ca^{2+} elicited an increase in the intracellular calcium level (Figure 2B), significantly higher than the control (p < 0.0001), which suggests that TMEM63B is a calcium-sensitive channel. To provide further support for our hypothesis, we also challenged HEK293T cells transfected with the TMEM63B-EGFP fusion protein with 150 mM mannitol, to simulate hypertonic shock, and evaluated $[Ca^{2+}]_i$ oscillation (Figure 2C). The increase in $[Ca^{2+}]_i$ induced by mannitol was significantly larger in cells transiently overexpressing TMEM63B-EGFP than in those expressing the empty vector (p < 0.0002) (Figure 2C,D). Exposing cells to a hypertonic solution is a form of mechanical stress that caused cells to retract (Figure 2E and Movies V1 and V2). Still, the importance of choosing cells that lack endogenous mechanically activated (MA) channels to assess the mechanotransduction properties is crucial. It is known that HEK293T cells possess the MA channels Piezo and NOMPC that can also induce MA currents,[21,22] yet it is clear that the transfected cells react to the mannitol shock; still this response is moderate relative to stimulation with $[Ca^{2+}]$ (Figure 2F,G and Movie V2). We also tested a higher mannitol concentration (300 mM), but the results were not significantly different (data not shown). Strikingly, a recent study confirmed *Mm*TMEM63B as mechanosensitive, inducing stretch-activated currents when expressed in naïve cells.[9] Systemic osmoregulation is a crucial process whereby changes in plasma osmolality, detected by osmoreceptors, modulate renal function and stabilize the tonicity and volume of the extracellular fluid.[7,23] Because TMEM63B shows distinct membrane expression in several cell types, being widely expressed in the kidneys (renal tubules), epididymis, lungs, and tonsils,[24] it is valid to assume that this channel might contribute to osmosensitive entry of Ca^{2+} into these tissues.

We also determined the localization of TMEM63B-EGFP (Figure 3A) by confocal microscopy, and the protein was found to be predominantly associated with the plasma membrane and cortical F-actin but not vinculin (Figure 3B and Figure S4).

It is known that the actin network is involved in several cellular processes related to the control of dynamic cellular morphology, organelle organization, and motility in reaction to various chemical and mechanical signals.[25] Dysfunction in proteins in the actin and focal adhesion proteomes is associated with numerous severe diseases, such as muscular disorders and cancers. Moreover, intracellular Ca^{2+} has a great impact on the migration machinery of healthy, tumor, and stromal cells.[26−28] On the basis of this combined information, the role of TMEM63B in HEK293T cells was thought to regulate cell migration. To demonstrate this, we transiently overexpressed the TMEM63B-EGFP fusion protein (Figure 4A) in HEK293T cells, which express a low level of TMEM63B (Figure 4B). We first applied a scratch and then evaluated by microscopy the cell wound closure and the ability of the HEK293T cells to migrate and subsequently close the wound made in a confluent plate of cells, after 24 h (see Figure 4C). On the basis of the width of the wound, we calculated the percentage of wound healing (Figure 4D). The tendency of HEK293T cells to detach from the plate immediately after the wound is made was prevented by coating with 0.1% gelatin. Remarkably, our data indicated that overexpression of TMEM63B-EGFP significantly increased the level of migration

DOI: 10.1021/acs.biochem.9b00224
Biochemistry XXXX, XXX, XXX−XXX

of HEK293T cells relative to control cells ($p < 0.02$). Cell migration is a central component of the metastatic cascade, which requires a concerted action of ion channels and transporters, cytoskeletal elements, and signaling. The migration cycle demands spatially synchronized changes of the actin cytoskeleton[28,29] in which TMEM63B might play an important role. We also evaluated the effect in wound healing of the cell permeant Ca^{2+} chelator bapta-AM. Treatment with the Ca^{2+} chelating agent caused some degree of cell detachment. Incubation of the cells with bapta-AM reduced the percentage of wound healing both for TMEM63B-EGFP-overexpressing cells and for the control (Figure 4E,F), which suggests the existence of a Ca^{2+}-dependent migration process. Studies have reported that several ion channels contribute to a variety of basic cell processes such as proliferation, adhesion, migration, and invasion by inducing local volume changes and/or by modulating Ca^{2+} influx, crucial for carcinogenesis and cancer development.[30,31] Interestingly, TMEM63B was one of the mRNAs, among a few others, for which expression appears to be downregulated by miR-199a-5p in mouse keratinocytes,[32] a small noncoding RNA molecule. These molecules mediate diverse biological cellular processes through regulatory pathways, targeting genes through translational repression or mRNA degradation.[33] Previous studies have also implicated the same miR-199a-5p gene targets in cell proliferation and migration in cancer cells. Intrigued by these data, we also evaluated TMEM63B mRNA expression in different cancer cell lines (lung, hepatocyte, and ductal carcinomas and breast adenocarcinoma). We found a differential gene expression among the different cell lines, the mRNA expression level of the T47-D cell line (ductal carcinoma) being >2-fold higher than that of HEK293T cells, as shown in Figure 4G.

In conclusion, our results indicate that the TMEM63B protein belongs to an osmosensitive ion channel family, which is conserved across eukaryotes, and has an architecture similar to that of the OSCA family. We show that expression of TMEM63B in HEK293T cells promotes $[Ca^{2+}]_i$ influx across the plasma membrane in response to extracellular $[Ca^{2+}]$ and hyperosmolarity. Moreover, overexpression of TMEM63B-EGFP enhances cell migration in HEK293T cells. These results directly demonstrate that TMEM63B is linked to Ca^{2+} signaling on which cell migration is dependent, which suggests for the first time such a functional role for TMEM63B. We are now focusing on the identification of the molecular mechanisms by which TMEM63B overexpression affects cell migration. Furthermore, we found an increase in the level of TMEM63B mRNA expression in the ductal carcinoma T47-D cell line, and we are conducting studies to clarify the potential role(s) of TMEM63B as a cancer biomarker.

■ ASSOCIATED CONTENT

Supporting Information

The Supporting Information is available free of charge on the ACS Publications website at DOI: 10.1021/acs.biochem.9b00224.

Detailed materials and methods and supporting figures (PDF)

Movie V1 (MP4)

Movie V2 (MP4)

Accession Codes

TMEM63B, Uniprot entry Q3TWI9.

■ AUTHOR INFORMATION

Corresponding Authors

*E-mail: gb453@cam.ac.uk or gbernardes@medicina.ulisboa.pt.

*E-mail: martamarques@medicina.ulisboa.pt.

ORCID

Sandra H. Vaz: 0000-0003-4258-9397

Gonçalo J. L. Bernardes: 0000-0001-6594-8917

Author Contributions

§M.C.M. and I.S.A. contributed equally to this work.

Funding

Funded by the Royal Society (URF\R\180019 to G.J.L.B.) and FCT Portugal (iFCT IF/00624/2015 to G.J.L.B., Postdoctoral Fellowships SFRH/BPD/118731/2016 to M.C.M. and SFRH/BPD/81627/2011 to S.H.V., and Doctoral Studentship SFRH/BD/111556/2015 to I.S.A.).

Notes

The authors declare no competing financial interest.

■ ACKNOWLEDGMENTS

The authors thank Dr. Vikki Cantrill for her help with the editing of the manuscript.

■ REFERENCES

(1) Saier, M. H., Jr, Reddy, V. S., Tsu, B. V., Moreno-Hagelsieb, G., Li, C., and Ahmed, M. S. (2016) The Transporter Classification Database (TCDB): recent advances. *Nucleic Acids Res. 44*, D372−D379.

(2) Medrano-Soto, A., Moreno-Hagelsieb, G., McLaughlin, D., Ye, Z. S., Hendargo, K. J., and Saier, M. H. (2018) Bioinformatic characterization of the Anoctamin Superfamily of Ca2+-activated ion channels and lipid scramblases. *PLoS One 13*, No. e0192851.

(3) Godzik, A., and Ye, Y. (2003) Flexible structure alignment by chaining aligned fragment pairs allowing twists. *Bioinformatics 19* (Suppl. 2), ii246−ii255.

(4) Jojoa-Cruz, S., Saotome, K., Murthy, S. E., Tsui, C. C. A., Sansom, M. S. P., Patapoutian, A., and Ward, A. B. (2018) Cryo-EM structure of the mechanically activated ion channel OSCA1.2. *eLife 7*, No. e41845.

(5) Zhang, M., Wang, D., Kang, Y., Wu, J.-X., Yao, F., Pan, C., Yan, Z., Song, C., and Chen, L. (2018) Structure of the mechanosensitive OSCA channels. *Nat. Struct. Mol. Biol. 25*, 850−858.

(6) Liu, X., Wang, J., and Sun, L. (2018) Structure of the hyperosmolality-gated calcium-permeable channel OSCA1.2. *Nat. Commun. 9*, 5060.

(7) Sharif-Naeini, R., Ciura, S., Zhang, Z., and Bourque, C. W. (2008) Contribution of TRPV channels to osmosensory transduction, thirst, and vasopressin release. *Kidney Int. 73*, 811−815.

(8) Zhao, X., Yan, X., Liu, Y., Zhang, P., and Ni, X. (2016) Co-expression of mouse TMEM63A, TMEM63B and TMEM63C confers hyperosmolarity activated ion currents in HEK293 cells. *Cell Biochem. Funct. 34*, 238−241.

(9) Murthy, S., Dubin, A., Whitwam, T., Jojoa-Cruz, S. J., Cahalan, S., Mousavi, S. A. R., Ward, A., and Patapoutian, A. (2018) OSCA/TMEM63 are an Evolutionarily Conserved Family of Mechanically Activated Ion Channels. *eLife 7*, No. e41844.

(10) Altschul, S. F., Gish, W., Miller, W., Myers, E. W., and Lipman, D. J. (1990) Basic local alignment search tool. *J. Mol. Biol. 215*, 403−410.

(11) Berman, H. M., Weissig, H., Shindyalov, I. N., Gilliland, G., Westbrook, J., Bourne, P. E., Bhat, T. N., and Feng, Z. (2000) The Protein Data Bank. *Nucleic Acids Res. 28*, 235−242.

(12) Nakamura, T., Tomii, K., Yamada, K. D., and Katoh, K. (2018) Parallelization of MAFFT for large-scale multiple sequence alignments. *Bioinformatics 34*, 2490−2492.

DOI: 10.1021/acs.biochem.9b00224
Biochemistry XXXX, XXX, XXX−XXX

(13) Little, D. Y., and Chen, L. (2009) Identification of Coevolving Residues and Coevolution Potentials Emphasizing Structure, Bond Formation and Catalytic Coordination in Protein Evolution. *PLoS One 4*, No. e4762.
(14) Waterhouse, A., Rempfer, C., Heer, F. T., Studer, G., Tauriello, G., Bordoli, L., Bertoni, M., Gumienny, R., Lepore, R., Bienert, S., de Beer, T. A P., and Schwede, T. (2018) SWISS-MODEL: homology modelling of protein structures and complexes. *Nucleic Acids Res. 46*, W296−W303.
(15) Dereeper, A., Guignon, V., Blanc, G., Audic, S., Buffet, S., Chevenet, F., Dufayard, J.-F., Guindon, S., Lefort, V., Lescot, M., Claverie, J.-M., and Gascuel, O. (2008) Phylogeny.fr: robust phylogenetic analysis for the non-specialist. *Nucleic Acids Res. 36*, W465−W469.
(16) McNally, D., and Fares, M. A. (2006) CAPS: coevolution analysis using protein sequences. *Bioinformatics 22*, 2821−2822.
(17) Shannon, P., Markiel, A., Ozier, O., Baliga, N. S., Wang, J. T., Ramage, D., Amin, N., Schwikowski, B., and Ideker, T. (2003) Cytoscape: A Software Environment for Integrated Models of Biomolecular Interaction Networks. *Genome Res. 13*, 2498−2504.
(18) DeLano, W. L. (2002) *The PyMOL Molecular Graphics System*, DeLano Scientific LLC, Palo Alto, CA.
(19) Webb, B., and Sali, A. (2016) Comparative Protein Structure Modeling Using MODELLER. *Curr. Protoc. Bioinf. 54*, 5.6.1−5.6.37.
(20) Glaser, F., Rosenberg, Y., Kessel, A., Pupko, T., and Ben-Tal, N. (2005) The ConSurf-HSSP database: The mapping of evolutionary conservation among homologs onto PDB structures. *Proteins: Struct., Funct., Genet. 58*, 610−617.
(21) Dubin, A. E., Murthy, S., Lewis, A. H., Brosse, L., Cahalan, S. M., Grandl, J., Coste, B., and Patapoutian, A. (2017) Endogenous Piezo1 Can Confound Mechanically Activated Channel Identification and Characterization. *Neuron 94*, 266−270.
(22) Coste, B., Mathur, J., Schmidt, M., Earley, T. J., Ranade, S., Petrus, M. J., Dubin, A. E., and Patapoutian, A. (2010) Piezo1 and Piezo2 Are Essential Components of Distinct Mechanically Activated Cation Channels. *Science 330*, 55−60.
(23) Bourque, C. W. (2008) Central mechanisms of osmosensation and systemic osmoregulation. *Nat. Rev. Neurosci. 9*, 519−531.
(24) Uhlen, M., Zhang, C., Lee, S., Sjöstedt, E., Fagerberg, L., Bidkhori, G., Benfeitas, R., Arif, M., Liu, Z., Edfors, F., Sanli, K., von Feilitzen, K., Oksvold, P., Lundberg, E., Hober, S., Nilsson, P., Mattsson, J., Schwenk, J. M., Brunnström, H., Glimelius, B., Sjöblom, T., Edqvist, P.-H., Djureinovic, D., Micke, P., Lindskog, C., Mardinoglu, A., and Ponten, F. (2017) A pathology atlas of the human cancer transcriptome. *Science 357*, No. eaan2507.
(25) Mitchison, T. J., and Cramer, L. P. (1996) Actin-based cell motility and cell locomotion. *Cell 84*, 371−379.
(26) Kunzelmann, K. (2005) Ion Channels and Cancer. *J. Membr. Biol. 205*, 159−173.
(27) Bose, T., Cieślar-Pobuda, A., and Wiechec, E. (2015) Role of ion channels in regulating Ca^{2+} homeostasis during the interplay between immune and cancer cells. *Cell Death Dis. 6*, No. e1648.
(28) Schwab, A., and Stock, C. (2014) Ion channels and transporters in tumour cell migration and invasion. *Philos. Trans. R. Soc., B 369*, 20130102.
(29) Ridley, A. J., Schwartz, M. A., Burridge, K., Firtel, R. A., Ginsberg, M. H., Borisy, G., Parsons, J. T., and Horwitz, A. R. (2003) Cell migration: integrating signals from front to back. *Science 302*, 1704−1709.
(30) Guilbert, A., Gautier, M., Dhennin-Duthille, I., Haren, N., Sevestre, H., and Ouadid-Ahidouch, H. (2009) Evidence that TRPM7 is required for breast cancer cell proliferation. *Am. J. Physiol. Cell Physiol. 297*, C493−C502.
(31) Himi, N., Hamaguchi, A., Hashimoto, K., Koga, T., Narita, K., and Miyamoto, O. (2012) Calcium influx through the TRPV1 channel of endothelial cells (ECs) correlates with a stronger adhesion between monocytes and ECs. *Adv. Med. Sci. 57*, 224−229.
(32) Kim, B.-K., Kim, I., and Yoon, S. K. (2015) Identification of miR-199a-5p target genes in the skin keratinocyte and their expression in cutaneous squamous cell carcinoma. *J. Dermatol. Sci. 79*, 137−147.
(33) Aalto, A. P., and Pasquinelli, A. E. (2012) Small non-coding RNAs mount a silent revolution in gene expression. *Curr. Opin. Cell Biol. 24*, 333−340.

DOI: 10.1021/acs.biochem.9b00224
Biochemistry XXXX, XXX, XXX−XXX